Ligand Receptor Dynamics at Streptavidin-Coated Particle Surfaces: A Flow Cytometric and Spectrofluorimetric Study

Tione Buranda,*,†,‡ Greg M. Jones,† John P. Nolan,§ Jan Keij,§ Gabriel P. Lopez,*,‡ and Larry A. Sklar*,†,§

Cancer Center and Department of Pathology, University of New Mexico School of Medicine, Albuquerque, New Mexico 87131; Chemical and Nuclear Engineering, and Department of Chemistry, University of New Mexico, Albuquerque, New Mexico 87131; and Life Sciences Division and National Flow Cytometry Resource, Los Alamos National Laboratories, Los Alamos, New Mexico 87545

Received: September 23, 1998; In Final Form: January 19, 1999

We have the studied the binding of 5-((*N*-(5-(*N*-(6-(biotinoyl)amino)hexanoyl)amino)pentyl)thioureidyl)-fluorescein (fluorescein biotin) to 6.2 μm diameter, streptavidin-coated polystyrene beads using a combination of fluorimetric and flow cytometric methods. We have determined the average number of binding sites per bead, the extent of fluorescein quenching upon binding to the bead, and the association and dissociation kinetics. We estimate the site number to be ≈1 million per bead. The binding of the fluorescein biotin ligand occurs in steps where the insertion of the biotin moiety into one receptor pocket is followed immediately by the capture of the fluorescein moiety by a neighboring binding pocket; fluorescence quenching is a consequence of this secondary binding. At high surface coverage, the dominant mechanism of quenching appears to be via the formation of nonfluorescent nearest-neighbor aggregates. At early times, the binding process is characterized by biphasic association and dissociation kinetics which are remarkably dependent on the initial concentration of the ligand. The rate constant for binding to the first receptor pocket of a streptavidin molecule is ≈$(1.3 \pm 0.3) \times 10^7$ M^{-1} s^{-1}. The rate of binding of a second biotin may be reduced due to steric interference. The early time dissociative behavior is in sharp contrast to the typical stability associated with this system. The dissociation rate constant is as high as 0.05 s^{-1} shortly after binding, but decreases by 3 orders of magnitude after 3 h of binding. Potential sources for the time dependence of the dissociation rate constant are discussed.

Introduction

Particulate surfaces are widely used as platforms for molecular recognition and assembly in sensors and other applications.[1] The binding of analytes to particles, either cells or beads, has been used in a wide variety of applications, including immunoassays, studies of protein−protein, protein−lipid, DNA−protein interactions, and enzymology.[2] In addition, bead-based platforms have found widespread use in chemosensing applications[3] and combinatorial chemistries[4−6] over the past few years. Beads functionalized with various chemical (or biological) groups are commercially available. Nevertheless, the interactions of beads and ligands have been incompletely characterized. The purpose of this work is to study such interactions in a model system and to determine the applicability of methods developed by ourselves[2,7−9] and others[10,11] to utilize this prototype for biosensing applications.

Many methods for constructing biomolecular assemblies at interfaces take advantage of the specific interaction between biotin and streptavidin or its congener avidin. Streptavidin consists of four subunits, each capable of binding biotin with high affinity.[12−20] The biotin−avidin binding, often cited as the strongest ($K_a \approx 10^{15}$ M^{-1})[14,21] known among noncovalent protein−ligand interactions, has been the subject of numerous studies, collateral with its use in wide ranging bioanalytical applications.[1,19−25]

We have studied the interactions of 5-((*N*-(5-(*N*-(6-(biotinoyl)-amino)hexanoyl)amino)pentyl)thioureidyl)fluorescein (referred to herein as fluorescein biotin) with streptavidin-covered polystyrene beads in a series of flow cytometric and spectrofluorimetric experiments. The beads are ideally suited for flow cytometry, which is uniquely capable of making ultrasensitive and quantitative fluorescence measurements with *in situ* discrimination of free from bead bound fluorophores. The streptavidin monolayer is covalently attached to the beads via a ($-(CH_2)_{10}-$) alkyl chain.[26] Because the streptavidin is coupled to the alkyl chain nonspecifically via a chemical reaction of any of the R-NH_2 groups at the protein surface, the spatial orientation of the binding pockets is presumed to be random (Figure 1). The fluorescein biotin ligand was selected because it has been well characterized[27] and has been determined to bind readily to streptavidin in solution.

We have examined the kinetics of ligand binding and release, and the mechanism by which binding results in fluorescence quenching. The early biotin/streptavidin binding dynamics are complex. The binding is characterized by biphasic association and dissociation kinetics which are unusually dependent on the initial concentration of the ligand. We attribute this behavior to a combination of factors: (a) heterogeneity in the degree of accessibility of receptors at the bead surface and (b) steric hindrance to incoming ligands from bead-resident ligands as surface coverage builds up.

Although the coupling of bulky substituents to biotin has been shown to reduce the strength and stability of the biotin/streptavidin bond,[19,21,28,29] the facile dissociation associated with

† University of New Mexico School of Medicine.
‡ University of New Mexico.
§ Los Alamos National Laboratories.

10.1021/jp983842h CCC: $18.00
Published on Web 04/15/1999

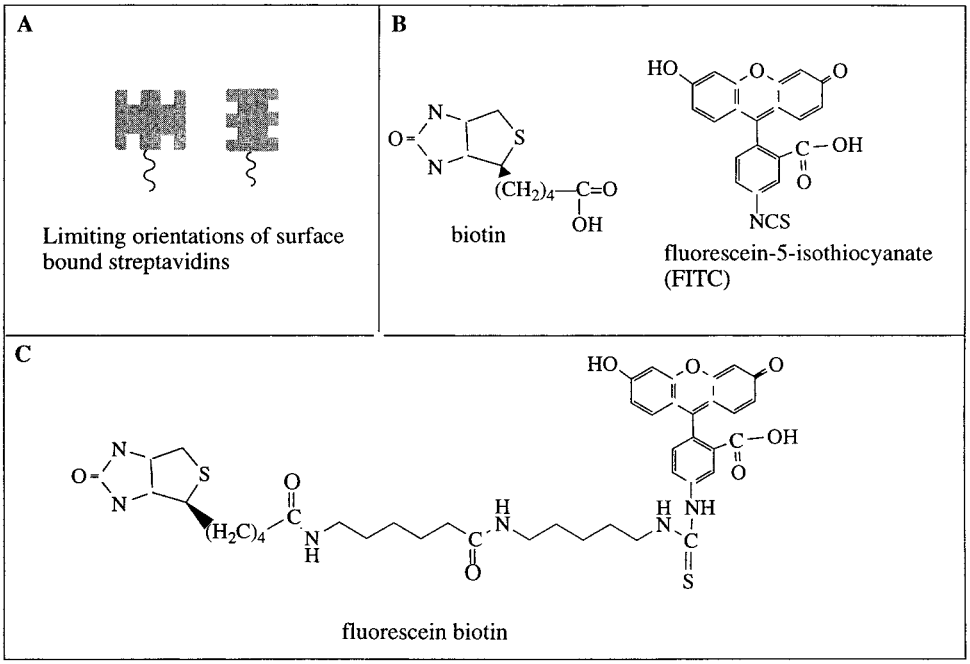

Figure 1. Schematic depiction of the streptavidin tetramer, showing binding sites randomly oriented at the surface. Also pictured are the molecular structures of native biotin, fluorescein isothiocyanate chromophore (FITC), and fluorescein biotin, 5-((*N*-(5-(*N*-(6-(biotinoyl)amino)hexanoyl)-amino)pentyl)thioureidyl)fluorescein.

short time incubations is in sharp contrast to the typical stability associated with this system. The dissociation rate constant of the complex was determined to be as high as 0.05 s^{-1} at early times after binding, and to decrease with contact time. Potential sources for the effect of time on the dissociation rate constant are identified.

Experimental Section

A. Materials. 6 μm diameter streptavidin-coated polystyrene beads (Spherotech Inc., Libertyville, IL) were obtained as 10% (w/v) suspensions according to the manufacturer's data sheet. Hemocytometric analysis of the beads revealed the numerical concentration of the particles to be in the range of $(4-5) \times 10^7$ beads/mL depending on the batch. Biotin and fluorescein biotin were purchased from Molecular Probes (Eugene, OR) and used without further purification. Polyclonal antifluorescein antibodies were prepared as described previously.[8]

B. Bead Suspensions. Bead suspensions, $\approx 10^6-10^7$ beads/mL , were prepared in a 100 mM tris, 300 mM NaCl buffer solution (pH 7.5) containing 0.1% bovine serum albumin (BSA). BSA adsorbs nonspecifically to the bead surface and is commonly used to block nonspecific binding sites at surfaces. Control bead suspensions were prepared in the same buffer solution with 0.1% BSA and 10^{-4} M native biotin, the latter being used to occupy specific sites, thus blocking subsequent binding interactions with fluorescein biotin. The native biotin is in the carboxylic acid form and is sparingly soluble in water, at low pH, or low ionic strength buffers. Accordingly, a high ionic strength buffer such as the one used here is desirable, for solubility and maintenance of proper pH. In parallel studies with peptide ligands, to be reported elsewhere,[30] the ionic strength of the buffer was varied from 10 mM to 1 M NaCl concentrations, with little effect on fluorescein biotin binding. We settled on the buffer containing 300 mM NaCl as the one most suitable for all experiments.

During the course of these studies, we observed that the apparent binding capacity of the beads, and the consistency of results, depend on the way the sample is handled prior to data collection. The stock bead suspension typically settles and aggregates during storage. Dispersion of bead aggregates was necessary for homogeneous assembly of fluorescein biotin throughout the bead population. This was accomplished by brief sonication or vortexing of the suspension prior to incubation in the ligand solution. Prolonged sonication ($\geq$1 min) appears to "strip" streptavidin sites from the bead surface. Furthermore, elevating the concentration of BSA or prolonging the exposure to BSA (several hours to days) tends to reduce the binding capacity of beads, possibly due to the eventual adsorption of BSA that results in blocking of biotin binding sites.

Reproducible data were obtained from samples that were pre incubated in the buffer with 0.1% BSA (typically for 20 min) and native biotin as needed. Equilibrium binding data were collected with the flow cytometer from samples that had been incubated with fluorescein biotin for an hour. For kinetic binding data, parallel samples were typically incubated in the presence or absence of free biotin for at least 30 min prior to use with fluorescent ligands. The samples, with or without biotin, were divided into 200 μL aliquots suitable for parallel kinetic analysis using the spectrofluorimeter and flow cytometer. Fluorimetric samples were placed in cylindrical cuvettes (SIENCO Inc., Morrison, CO). The cuvettes were put into an adapter designed to fit into a temperature-controlled sample holder, equipped with a motor for sample stirring (using 2 $\times$ 5 mm stir bars, Bel-Art, Paquannock, NJ). Instrument details and protocols have been described elsewhere.[7,8] Flow cytometric samples were put into 12 $\times$ 75 mm Falcon tubes (Becton Dickinson Labware, Lincoln Park NJ).

C. Binding Analysis of Fluorescein Biotin and Streptavidin-Bearing Beads. *1. Spectrofluorimetry.* Spectrofluorimetric measurements were performed in single photon counting mode on an SLM-Aminco 8000 spectrofluorimeter (SLM Instruments, Rochester, NY). The sample was excited at 490 nm, with a 10 nm band-pass interference filter (Corion Corp., Holliston, MA)

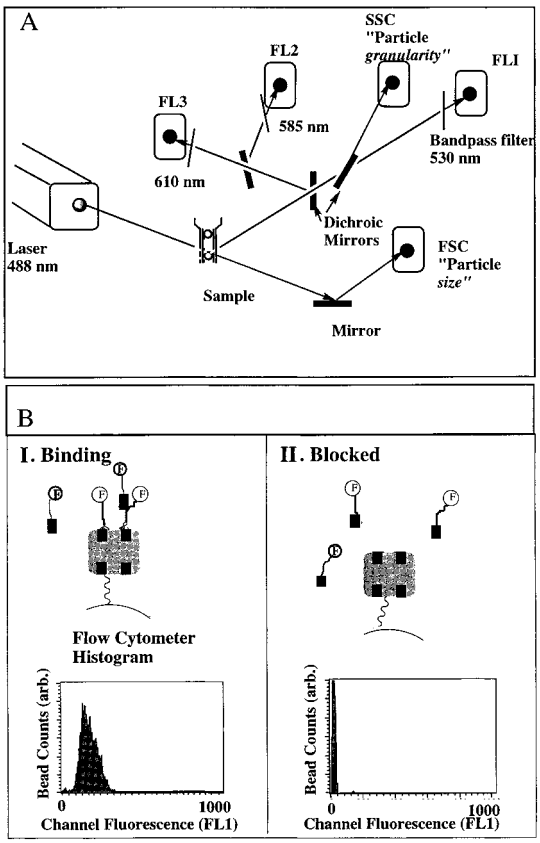

Figure 2. (A) Schematic representation of the flow cytometric detection system. Analyses are triggered by light scattered at forward angles and gated on the basis of forward (FSC) and right angle scatter (SSC) selecting for beads. Thus, the flow cytometer can distinguish between free and bound ligand. Fluorescence from bead-bound ligand is detected at FL1 which is optimized for fluorescein luminescence. (B) Control of specific and nonspecific binding sites: (I) BSA blocks nonspecific binding sites on the bead surface while fluorescein biotin binds specifically to streptavidin binding sites. Binding is detected by measurement of fluorescence emission at FL1. The histogram shows a typical distribution of fluorescence intensity (along *x* axis) measured for the bead populations sampled. (II) Native biotin blocks specific sites on bead. Thus, no ligands can bind and no luminescence is observed, as indicated by the histogram.

used for line narrowing and stray light rejection. Fluorescein emission was monitored at 520 nm via a long-pass band filter (3-70 Kopp Glass, Pittsburgh, PA) and a 520 nm (10 nm band-pass) filter (Corion Corp). Neutral-density filters were used to keep light intensities of the brightest samples within the phototube dynamic range.

2. Flow Cytometry. The flow cytometric analysis used a Becton-Dickinson FACScan flow cytometer (Sunnyvale, CA) interfaced to a Power PC Macintosh using the CellQuest software package. The FACScan is equipped with a 15 mW air-cooled argon ion laser. The laser output is fixed at 488 nm. The detection scheme uses five detectors: (a) two scatter channels at forward and right angles to the incident light (FSC and SSC in Figure 2), which are triggered when particles of a given size (e.g., 6 μm beads) pass through the laser beam, and (b) three photomultiplier tubes dedicated to fluorescence detection at fixed wavelengths of 530, 585, and 610 nm (FL1, FL2, and FL3, respectively, in Figure 2A). Fixed band-pass filters are used for wavelength selection and are optimized for the desired emission. As fluorescein biotin specifically binds to streptavidin at bead surfaces (Figure 2B (I)) the data are displayed as a histogram corresponding to the fluorescence in channel 1 (FL1) for the bead population. For beads with blocked receptor sites (Figure 2B (II)), the fluorescence histogram such as the one displayed is typically comparable to bead scatter in neat buffer. However, in the case of relatively high supernatant concentrations (100−300 nM) of fluorescein biotin, the onset of nonspecific binding is apparent in the modest fluorescence intensity displayed by blocked beads.

The critical feature that makes flow cytometry a powerful tool for study of ligand−receptor interactions is its ability to discriminate free from bound fluorescein biotin. This capacity depends on the measurement of fluorescence specifically associated with the bead as it is illuminated by the laser beam. Typically, flow cytometric fluorescence data are acquired only when the detection electronics are triggered by a light scatter signal indicating the presence of a bead. If the sample stream and/or the laser beam diameters are sufficiently small, the fluorescence from free ligand in the sample volume surrounding the bead is negligible compared to the signal from bound ligand[31] concentrated on the bead surface. To analyze the binding data, the bead histograms were evaluated. It has been shown elsewhere[9] that the mean of the histogram is the quantity relevant to binding capacity. The average fluorescence on a single bead is converted to the number of fluorophores per bead on the basis of flow cytometric calibration beads (Quantum 825 Flow Cytometry Standards Corp., San Juan, PR). Thus, conversion from mean channel fluorescence of histograms to the total bound ligand, $[LS]_t$ is shown in eq 1.[9]

$$[LS]_t = \frac{MCF_{LS}}{MCF_{std}} MESF \frac{1}{\Phi_L} \frac{1}{\phi_b} \frac{n}{A} \qquad (1)$$

MCF_i (mean channel fluorescence) are the means of the histograms of the bound ligand (LS, corrected for nonspecific binding) and calibration beads (std) read at similar detection settings. MESF (mean equivalent of soluble fluorophores) is the number of fluoresceins whose emission intensity is equal to MCF_{std}, on each bead. The MESF is based on native fluorescein. Thus, Φ_L is the emission yield of free fluorescein biotin relative to native fluorescein. ϕ_b is the quantum yield of bound fluorophores as evaluated from eq 3 or centrifugation assay data *(vide infra). n* is the number of beads per liter and *A* is Avogadro's number.

3. Calibration of Flow Cytometry Standard Beads. Due to uncertainty in the manufacturer-supplied MESF values we carried out a calibration of the standard beads. The mean equivalents of soluble fluorophores of calibration beads were determined by comparison to solutions of fluorescein. For clarity, the details are given in footnotes to Table 1.

4. Centrifugation Assay. Samples containing $\approx 8 \times 10^6$ beads/mL were incubated in 0.3−300 nM fluorescein biotin in Eppendorf tubes for at least an hour. In addition, an analogous bead-free set of fluorescein biotin solutions was prepared as controls. The bead suspensions were centrifuged for 5 min and the supernatants were collected in cylindrical cuvettes in preparation for fluorescence intensity measurements. The beads were resuspended in buffer. A small fraction of the beads (≈5%) was removed from each sample and used for flow cytometric analysis. The rest were used for spectrofluorimetric lifetime measurements. The paired intensities of residual supernatants (0.3−300 nM) were used to determine the concentration of fluorescein biotin associated with the beads ([LS]; see eq 2a). In eq 2a, I_0 and I_r are the fluorescent intensities of supernatants previously exposed to blocked and unblocked beads, respectively, and $[L]_0$ is the initial concentration of fluorescein biotin.

TABLE 1: Calibration of FSC 825 Beads (Batch No. A02609)

sample	intensity[c]	beads/mL[d]	MESF[e]
buffer	40		
825-0[a]	70	96×10^6	
825-1[a]	440	5.8	1.69×10^4
825-2[a]	1.0×10^3	6.4	3.11×10^4
825-3[a]	4.0×10^3	7.0	1.35×10^5
825-4[a]	1.2×10^4	9.2	3.55×10^5
2.10×10^{-7} M fl[b]	5.49×10^5		
4.20×10^{-8} M fl[b]	1.06×10^5		

[a] 1 mL aliquots of bead samples 825-(0-5) (representing incremental quantities of fluorophores/bead) were placed in Eppendorf tubes, centrifuged, and the supernatant decanted. The beads were resuspended in 320 μL of 100 mM Tris buffer (300 mM NaCl), for an hour. 300 μL volumes were transferred to cylindrical cuvettes for spectroscopic measurements. [b] Fluorescein dissolved in Tris buffer. The concentration was determined from absorption measurements. [c] Under comparable spectroscopic conditions as described in the text, fluorescence intensities and scatter from beads (photons/s), neat buffer, and fluorescein solutions were determined. [d] Analysis on a hemocytometer. [e] Mean equivalents of soluble fluorescein: intensity from the scatter of blank (nonfluoresceinated) sample, 825-0, is used as the baseline. Then the fluorescence intensity of the native fluorescein of known concentration is used to convert the intensities of the respective bead emissions to MESF.

$$[\mathrm{LS}] = \frac{I_0 - I_r}{I_0}[\mathrm{L}]_0 \tag{2a}$$

$$\text{sites} = [\mathrm{LS}]A/n \tag{2b}$$

The number of fluorophores per bead was determined from eq 2b, where A represents Avogadro's number and n is the number of beads per liter.

5. Spectrofluorimetric Analysis of the Kinetics of Fluorescein Biotin Binding to and Dissociation from Beads. In Situ Resolution of the Concentration of Free and Bound Ligand. This assay has been previously described for the binding of fluorescent ligands to receptors on suspended cells.[7-9] 200 μL aliquots of $\approx 8 \times 10^6$ beads/mL (in the presence or absence of native biotin) were placed into stirred cylindrical cuvettes for fluorescence measurements as described above. Fluorescence was monitored continuously during addition of fluorescein biotin (L) and, subsequently, antifluorescein antibody (Ab) to the stirred cuvettes through the top of the sample compartment using Hamilton syringes (Reno, NV). The progress of a typical reaction is illustrated in Figure 3. After a 15 s baseline was established, fluorescein biotin (e.g., 2 μL of 3.0×10^{-7} M) was added at t_0. In the absence of biotin, binding results in partial quenching of the fluorescence as shown in curve I. In the presence of excess biotin, the association of fluorescein biotin with the bead is virtually blocked. The fluorescence intensity (I_0) is essentially unchanged between the time fluorescein biotin is added at t_0(L) to the time the antibody is added at t_1(Ab). Binding was allowed to proceed for the desired time, and then a high affinity antibody ($K_a \approx 10^{10}$ M^{-1}) to fluorescein[8] was added to the cuvette (2 μL of $\approx 2.5 \times 10^{-6}$ M), at t_1. The antibody binds to free fluorescein biotin and quenches it at a rate close to the diffusion limit ($k_{diff} \approx 10^9$ M^{-1} s^{-1}). In contrast, the encounter between the antibody and the bead associated ligands is markedly slower being on the order of $\approx 10^5$ M^{-1} s^{-1}.[9] The antibody has an intrinsic quenching efficiency of $\approx$ 95%,[8] thus fluorescein biotin always displays residual fluorescence (R) whether free or bound. By visual inspection of curve I relative to II it is possible to quantify the amounts of free ($[\mathrm{L}]_t$; F on curve I) and bound ligand ($[\mathrm{LS}]_t$, B) at t_1(Ab). The evolution of the mixture of $[\mathrm{L}]_t$ and $[\mathrm{LS}]_t$ as represented by

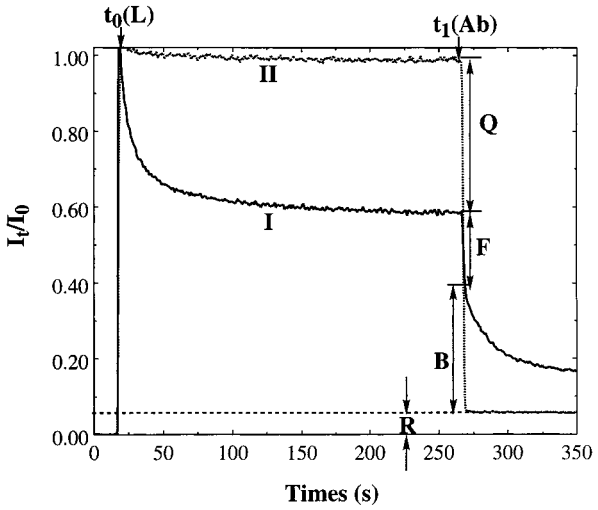

Figure 3. Spectrofluorimetric measurement of ligand binding and quenching on beads. Beads were monitored in stirred cuvettes in the absence (I) and presence (II) of native biotin. 15 s after data collection was initiated, fluorescein biotin was added, t_0(L); after 250 s t_1(Ab), an antibody to fluorescein was added which quenched free and bound ligand fluorescence. Q represents the quenching associated solely with binding of fluorescein biotin to the beads. $F_{(I)}$ represents the quenching of residual unbound ligand (L_t) and B represents the bound ligand (LS_t) that is quenched relatively slowly via diffusive encounter with the antibody. R represents the intrinsic residual fluorescence due to the incomplete quenching by the antibody.

I_t/I_0 in eq 3, is the result of the lower emission quantum yield of the bound species (ϕ_b) relative to the free.

$$\frac{I_t}{I_0} = \frac{[\mathrm{L}]_t}{[\mathrm{L}]_0} + \phi_b \frac{[\mathrm{LS}]_t}{[\mathrm{L}]_0} \tag{3}$$

It is important to note that this assay can readily resolve free and bound fluorescein biotin as long as the concentration of fluorescein biotin is less than the site concentration. When the concentration of fluorescein biotin is much greater than that of the binding sites, the resolution is lost because smaller fractions of fluorescein biotin are bound to the beads, and are harder to resolve due to their weak luminescence, relative to $[\mathrm{L}]_t$. In addition, at higher surface coverages of fluorescein biotin, bound ligands are quenched more rapidly via sequential engagement of neighboring fluorophores by the two F_{ab} arms of the antibody.[32]

6. Kinetic Model. The kinetic evolution of $[\mathrm{LS}]_t$(=LS + L_2S) was fit to a reversible binding model shown in eq 4. L and S represent fluorescent ligands and streptavidin receptor sites, respectively. L_2S represents streptavidin molecules that have bound two fluorescent ligands or two ligands bound to different streptavidin moieties, but in close enough proximity such that nearest-neighbor ligand interactions are expected to lead to lower fluorescence yields as well as slower binding kinetics *(vide infra)*. k_i are the binding rate constants, and k_{-i} are the dissociation rate constants. The coupled differential equations arising from eq 4 are solved numerically using commercial software (Scientist, Micromath Scientific Software, Salt Lake City , UT).

$$\mathrm{L} + \mathrm{S} \underset{k_{-1}}{\overset{k_1}{\rightleftharpoons}} \mathrm{LS} \tag{4a}$$

$$\mathrm{L} + \mathrm{S} \underset{k_{-2}}{\overset{k_2}{\rightleftharpoons}} \mathrm{L_2S} \tag{4b}$$

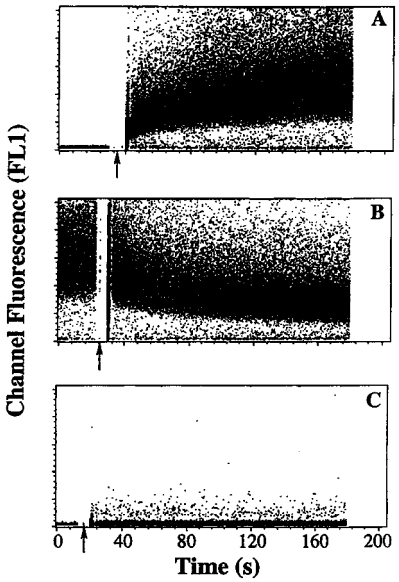

Figure 4. Kinetic analysis of binding of 1.5 nM fluorescein biotin to $\approx 8 \times 10^6$ beads/mL by flow cytometry: (A) time-resolved increase in bead luminescence intensity as more fluorescein biotin binds; (B) addition of native biotin leads to dissociation of ligand from bead as indicated by loss in intensity; (C) blocked sample, showing negligible bead associated fluorophores.

7. Static Flow Cytometric Analysis of Ligand Binding and Dissociation. Flow cytometric data were typically collected on equilibrated samples prepared in the presence and absence of biotin. In addition, sets of experiments were done in parallel with spectrofluorimetric kinetic analysis as described above. Typically, fluorescein biotin was incubated with stirring, for time intervals equal to the t_0(L) to t_1(Ab) span, before being analyzed with the flow cytometer.

8. Kinetic Cytometric Analysis, The time course of association was measured by acquiring a 10 s baseline, adding an aliquot of fluorescein biotin to the sample, briefly vortexing, and resuming data collection to completion at some desired time (e.g., 200 s). Dissociation rates were measured by interrupting a binding experiment after a given time (e.g., 60−1200 s, 2 h), then adding excess biotin, and resuming data collection. Progressive binding of the fluorescein biotin is indicated by the increasing brightness of the particles as they pass through the path of the laser (Figure 4A) and dissociation from the beads, initiated by the addition of native biotin is marked by decreasing brightness (Figure 4B). The raw data were converted to ASCII format, suitable for kinetic fitting, using software developed by Mr. Larry Seamer at UNM. The time-resolved change in bound fluorescence was then fit by nonlinear regression methods using the software package, GraphPad Prism (GraphPad Software, San Diego, CA).

D. Lifetime Measurements of Ligands and Beads. *1. Spectrofluorimetry.* Fluorescence lifetimes were measured using a frequency domain multiharmonic frequency fluorescence lifetime instrument, SLM 4850 MHF spectrofluorimeter (SLM Instruments, Rochester, NY) operated at 4−200 MHz. Excitation was provided by a pulse-modulated (4 MHz) cw argon ion laser operated at 488 nm (Model AP532, Omnichrome, Chino, CA). Sample fluorescence was detected through a long-pass band filter (3-70 Kopp Glass, Pittsburgh, PA) and a 520 (10 nm band-pass) filter (Corion Corp.). Experiments were performed at 25 °C in stirred cylindrical glass cuvettes similar to those used above. Excited state lifetimes were measured for fluorescein, fluorescein isothiocyanate (FITC), and fluorescein biotin. In addition, bead suspensions prepared in parallel with equilibrium intensity measurements were analyzed in 200 μL volumes. The fluorescence of fluorescein biotin bound to 10^7 beads/mL provided adequate signal-to-background for analysis. In frequency domain measurements, the observable parameters are the phase difference (ϕ), between the pulse modulated excitation wave and the emitted photons, and the amplitude demodulation (m) between the incident and emitted light. [33] For a solution of fluorophores, phase (τ_p) and modulation (τ_m) derived lifetimes arise from eq 5.

$$\tan \phi = \omega \tau_p, \quad \tau_p = \omega^{-1} \tan \phi \tag{5a}$$

$$m = [1 + \omega^2 \tau_m{}^2]^{-1/2}, \quad \tau_m = \omega^{-1}[m^{-2} - 1]^{1/2} \tag{5b}$$

ω spans the range of modulation frequencies from 4 to 200 mHz.

The phase shift of the fluorescence signal was measured with reference to the scattered signal ($\tau = 0$ ns) from a suspension of oyster glycogen in Tris buffer. Data analysis was performed using a nonlinear least-squares routine for fitting experimental lifetimes supplied by the manufacturer. The default values were used as the uncertainties in the measured phase angle (0.5°) and modulation amplitude (0.5%).

2. Flow Cytometric Lifetime Measurements. Phase-sensitive flow cytometric measurements were performed at Los Alamos National Laboratory. The details of the experimental principles[34] and measurement are described elsewhere.[35,36] Briefly, samples were excited at 488 nm by a sinusoidally modulated (29 MHz) cw beam from an argon ion laser (Model 2025, Spectra Physics, Palo Alto, CA). Sample fluorescence was transmitted through a long-pass filter (OG 515, Melles Griot, Irvine, CA) and detected with a PMT. The modulated fluorescence signal was processed by analog phase-sensitive detection electronics to obtain the phase-shift and lifetime at 29 MHz.

E. Fluorescence Intensity, Polarization, and Lifetime Analysis with Soluble Streptavidin. Experiments were performed under the same spectroscopic conditions as described above to examine binding of soluble fluorescein biotin to streptavidin in solution. In a typical experiment, cuvettes containing 200 μL of 1 nM fluorescein biotin in buffer were placed into the steady state (SLM 8000) and lifetime spectrofluorimeters (SLM 4850), respectively. Intensity and lifetime measurements were acquired before and after the addition of (e.g. 2 μL of 3 μM) soluble streptavidin , then again after the addition of an excess of biotin (0.5 μL, 10^{-3} M). Polarization data (P) of neat fluorescein biotin and that mixed with streptavidin were determined from intensity data measured with Glan-Thompson calcite prism polarizers placed in the excitation and emission paths. The system was calibrated using excitation scatter from a dilute solution of glycogen and data were collected following standard protocols.[33] Emission was detected at parallel ($I_{||}$) and perpendicular ($I_{\perp}$) orientations relative to vertically polarized excitation, and analyzed using eq 6.

$$P = \frac{I_{||} - I_{\perp}}{I_{||} + I_{\perp}} \tag{6}$$

Results

A. Analysis of Equilibrium Binding of Fluorescein Biotin to Beads. *1. Centrifugation Assay by Spectrofluorimetry.* The results of spectrofluorimetric analysis of supernatant solutions obtained by centrifugation are shown in Figure 5. At maximum

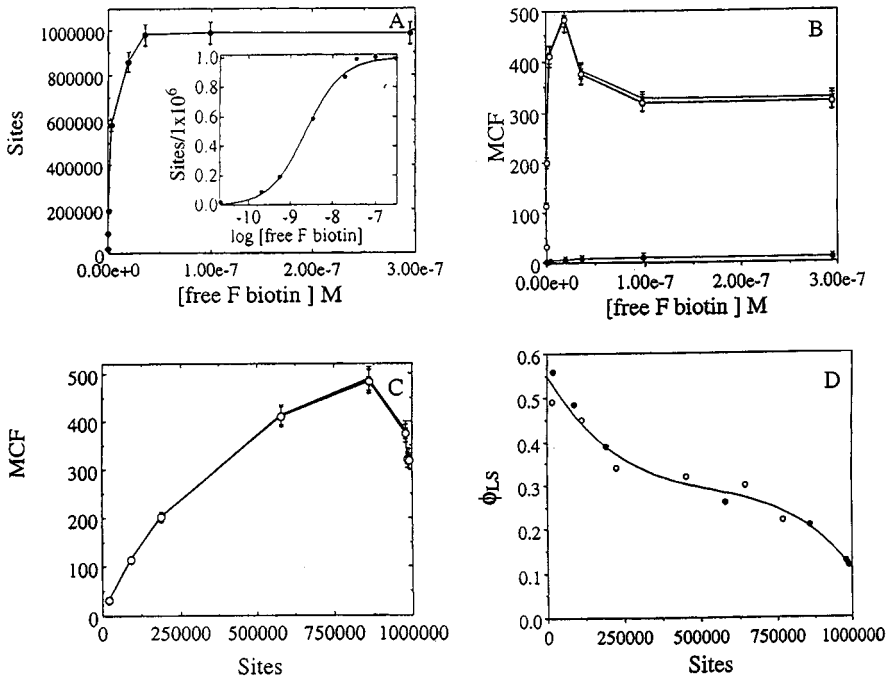

Figure 5. Equilibrium binding analysis on beads. (A) Equilibrium binding (occupied sites) of fluorescein biotin to beads versus free ligand concentration, as determined by the centrifugation assay using 8.0×10^6 beads/mL. Each point represents an average from three determinations. Insert: sigmoidal binding analysis ($R^2 = 0.99$) of binding data ($K_a \approx (4.3 \pm 0.2) \times 10^8$ M^{-1}). (B) Mean channel fluorescence (MCF) intensities of beads incubated in fluorescein biotin solutions versus free ligand concentrations. Asterisks represent total binding. Open circles represent specific binding only. Filled circles represent nonspecific binding. (C) Mean channel fluorescence of beads as a function of number of bound fluorophores. (D) Dependence of ϕ_b on the number fluorophore-occupied sites per bead. Open circles represent data from spectrofluorimetric analysis (cf. Figure 3), and filled circles represent centrifugation assay and flow cytometry data. The curve represents a theoretical fit to the cubic equation (eq 7).

surface coverage, approximately one million ligand molecules were bound. A plot of bound fluorophores versus log [free fluorescein biotin] (Figure 5A insert) gives a $K_a \approx (4.3 \pm 0.2) \times 10^8$ M^{-1}. This value is 5 orders of magnitude lower than that reported for native biotin and streptavidin, but is in the same range as reported for biotinylated DNA binding to streptavidin coated latex beads.[10]

2. Flow Cytometric Analysis of Binding. The fluorescence of the beads in the equilibrium assay was determined by flow cytometry. In order to elucidate how the fluorescence varies as a function of bound ligand concentration, the data is displayed in several different ways. In Figure 5B, with increasing amount of ligand in solution, and hence, increasing quantity of bound ligand, the fluorescence intensity increases and then decreases. Next, the mean channel fluorescence of the beads is plotted versus the mean number of occupied fluorophore sites/bead (Figure 5C). Finally, ϕ_b was plotted versus occupied sites (Figure 5D) thus displaying the dependence of the emission yield of bound fluorophores on occupancy.

3. Calibration of Flow Cytometric Binding Data by Standard Beads. Determination of ϕ_b. In the absence of quenching, (i.e., $\phi_b = 1$) eq 1 can be used to determine the number of fluorophores per bead, using data from standard beads of known calibration (Table I). However, as is the case here, bound ligands tend to be less luminous than their supernatant counterparts. ϕ_b can be determined using two methods, one which relies on the centrifugation assay and the other which relies on the antifluorescein antibody assay. The centrifugation method involves the calculation of fluorophores per bead using calibration beads. The numerical details are shown in footnotes c−e of Table 2.

The antifluorescein antibody assay (Figure 3) enables the paired determination of $[LS]_t$ and ϕ_b in a single experiment. Thus, in experiments where this analysis is done in parallel with flow cytometry (see Experimental Section, C3), ϕ_b from this assay can be used to determine $[LS]_t$ from flow cytometric analysis. The agreement between these ϕ_b data and those from the centrifugation assay, is displayed in (Figure 5D). The data show the dependence of ϕ_b on surface density, thus indicating the need for an empirical formalism to represent ϕ_b in a kinetic analysis. It was determined that the data in Figure 5D could be readily fit with a cubic polynomial.

$$\phi_b = (0.53 - 8.60) \times 10^7[LS + L_2S] + 1.09 \times 10^{16}[LS + L_2S]^2 - 5.26 \times 10^{23}[LS + L_2S]^3 \quad (7)$$

TABLE 2: Equilibrium Binding Data for Fluorescein Biotin to Streptavidin-Covered Beads: Comparison of Flow Cytometric Analysis and Spectrofluorimetric Analysis of Residual Supernatant

			ligands/bead ($\times 10^5$)		
	MCF[b]				
$[L]_0$ (nM)[a]	I	II	calib beads[c]	centrifugn assay[d]	ϕ_b[e]
0.3	31.0 ± 1.0	1.0	0.11 ± 0.003	0.21 ± 0.01	0.52
1.4	114.0 ± 6.0	1.0	0.44 ± 0.023	0.90 ± 0.04	0.49
3.1	201.0 ± 10.0	2.0	0.74 ± 0.037	1.90 ± 0.10	0.39
11.2	410.0 ± 20.0	3.0	1.51 ± 0.074	5.80 ± 0.29	0.26
30.8	482.0 ± 24.0	6.0	1.79 ± 0.089	8.60 ± 0.43	0.21
49.0	375.0 ± 18.0	7.0	1.24 ± 0.060	9.80 ± 0.49	0.13
112.0	318.0 ± 16.0	9.0	1.15 ± 0.058	9.90 ± 0.50	0.12
308.0	320.0 ± 16.0	13.0	1.19 ± 0.067	9.85 ± 0.50	0.12

[a] Initial concentration of supernatant fluorescein biotin ligand, determined from absorption: $\epsilon \approx 76\,000$ M^{-1} cm^{-1}. [b] Background corrected mean channel fluorescence (MCF) of histograms for bound (I), and native biotin-blocked (II) samples. See text for details. [c] Number of ligands per bead. Flow cytometric analysis: sites = $(MCF_{LS}/MCF_{std}) \times MESF \times (1/\Phi_L)$, where $\Phi_L \approx 0.82$ determined from fluorescent lifetime measurements, see text for details. [d] See eq 2 in text. [e] $\phi_b = sites_{mesf}/sites_{centrifuge}$.

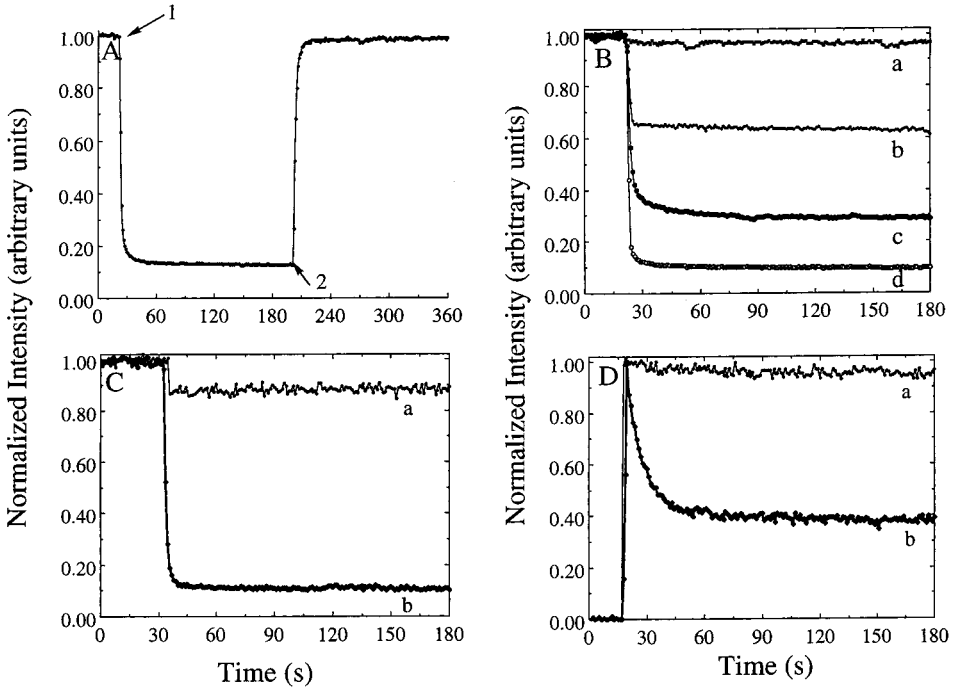

Figure 6. Quenching of biotin by streptavidin in solution. (A) Fluorescence emission intensity of 1.5 nM fluorescein biotin. Point 1: Injection of 68.0 nM soluble streptavidin. Point 2: Fluorescence recovery after addition of excess (10^{-5} M) native biotin. (B) The quenching effect of various concentrations of streptavidin (on 1.5 nM fluorescein biotin) where (a) 0.08 nM; (b) 1.66 nM; (c) 8.0 nM; (d) 68.0 nM. (C) Quenching related to the association of (a) 1.5 nM native FITC and (b) 1.5 nM fluorescein biotin, to 68 nM soluble streptavidin. (D) The association of FITC with the streptavidin binding pocket is mediated by biotinylation: (a) 1.5 nM native FITC alone does not significantly interact with 8×10^6 beads/mL and is thus not quenched. (b) 1.5 nM fluorescein biotin binds to beads and the fluorophore is quenched.

The first coefficient, 0.53, represents the amount of quenching associated with binding of fluorescein biotin to an isolated streptavidin on a bead. The other coefficients are determined from the fit.

B. Quenching, Polarization, and Lifetime Data. *1. Quenching*. Fluorescein biotin is quenched up to 90% when increasing amounts of soluble streptavidin are added (Figure 6A). However, when native biotin was added to the mixture, the fluorophore recovered 100% of its original luminescence intensity. The recovery of fluorescence is caused by the dislodging of fluorescein from proximal binding pockets. However, the biotin extremity of the ligand remains attached *(vide infra).* Figure 6B depicts the effects of titrating soluble streptavidin to fluorescein biotin. Incomplete quenching at stoichiometric or low excess quantities of streptavidin implicates a low equilibrium constant ($K_a \approx 1 \times 10^9$ M^{-1}). Figure 6, C and D, shows experiments which were designed to demonstrate that primary binding to receptor pockets (on beads) by fluorescein biotin is exclusive to the biotin moiety. Here, equimolar amounts (1.5 nM) of native fluorescein and fluorescein biotin were mixed to paired samples of soluble streptavidin (272 nM binding capacity), and beads (13 nM total binding capacity). The native fluorescein is moderately quenched (10%) in excess soluble streptavidin and is unquenched on beads compared to the fluorescein biotin. This observation is relevant to the kinetic analysis which is predicted on the biotin moiety being solely responsible for primary binding to the beads.

2. Polarization. Fluorescence radiation from small molecules is largely depolarized due to rotational diffusion. The relatively slow rotation of high molecular weight species allows the emitted radiation to remain partially polarized. Because of its relatively small size, fluorescein biotin (MW 831.01 g/mol) yields a small polarization value of 0.02. Upon complexation to streptavidin (MW 60 000 g/mol), polarization increases up to 10-fold yielding values of 0.12 in the 10% unquenched state, and 0.20 after the addition of excess native biotin. The polarization data fall within the range of the literature values for free and (strept)avidin-bound fluorescein biotin.[37,38] For comparison, our data is consistent with the literature measurements taken when the protein was in excess of the fluorophore. This condition ensures minimal contribution from free ligand. Because of the relatively larger molecular weight of avidin (MW 67 000−68 000 g/mol), avidin complexes had higher polarization values (≈ 0.20)[37,38] than streptavidin (0.12).[37]

3. Spectrofluorimetric Lifetime Measurements and Analysis. The fluorescence lifetimes measured before and after mixing with streptavidin, as well as after the subsequent addition of native biotin, were largely the same (Table 3). The lifetimes were generally fit to a two-component model. The lifetimes of the soluble ligands were largely monophasic (amplitude, $\alpha_1 \geq 0.98$). Attachment of biotin to fluorescein isothiocyanate results in $\approx$ 18% decrease in the lifetime relative to the native FITC.[9] Fluorophore lifetimes were only moderately diminished upon association with the beads. Beads with at least 1.9×10^5 fluorophores per bead were determined to have useful signal to noise. At coverages ranging from 1.9×10^5 to 9.85×10^5 fluorophores per bead, the measured lifetimes appeared to be dominated by longer lifetimes (isolated fluorophores) because the nearest-neighbor-quenched fluorophores are potentially so dim that they can not be detected and lifetimes are largely unchanged from sample to sample. A typical lifetime is shown in Table 3 for 5.85×10^5 fluorophores/bead.

In general, lifetime measurements in scattering media such as suspended beads are susceptible to inaccuracies due to excitation scatter leaking through to the detector.[39] We have, however, determined that the light scatter (putative lifetime of 0 ns) from the beads at concentrations used herein, (see *c* in Table 3 footnotes) was too small to affect the measured lifetimes of fluorescein biotin on beads.

TABLE 3: Excited State Lifetimes of Fluorescein, Fluorescein Isothiocyanate (FITC), and Fluorescein Biotin (F biotin) in Solution and on Beads As Measured by Spectrofluorimetry and Flow Cytometry[a]

Spectrofluorimetry

	lifetimes				
sample	τ_1 (ns)	α_1	τ_2 (ns)	α_2	τ_{av}[e]
fluorescein	3.96	0.99	0.38	0.01	3.96 ± 0.04
FITC	3.91	0.98	0.26	0.02	3.84 ± 0.02
fluorescein biotin	3.34	0.99	0.12	0.01	3.29 ± 0.05
F biotin + streptavidin[b]	3.39	0.94	0.57	0.06	3.15 ± 0.16
F biotin + blocked beads[c]	3.26	1.00			
5.80×10^5 F biotins/bead[d]	3.23	0.71	0.90	0.29	2.50 ± 0.15

Flow Cytometry[f]

F biotins/bead ($\times 10^5$)	τ_{29}
0.21	2.18
0.90	2.49
1.90	2.45
5.80	2.40
8.60	2.45
9.85	1.55

[a] Measurements were typically taken of 200 μL, 1.5 nM ligand solutions. For bead suspensions, $\approx 1.0 \times 10^7$ beads/mL were used. [b] Lifetime of residual fluorescence ($\approx$10%) of 1.0 nM fluorescein biotin after mixing with 68.0 nM soluble streptavidin as in Figure 6. [c] 2×10^7 beads/mL, blocked with native biotin, suspended in 1.5 nM fluorescein biotin solution. [d] Representative lifetime measurement of F biotin on beads. Detection was limited to beads with at least 1.9×10^5 F biotins/bead [e] Average multiharmonic frequency fluorimetric lifetimes (τ_{av}) are of at least three measurements. [f] Flow cytometric lifetimes (τ_{29}) were measured at 29 mHz. Because of a more powerful laser and the ability to focus excitation on a single bead, data was collected on samples which were below the detection limits of the spectrofluorimeter.

4. Phase-Sensitive Flow Cytometry. The phase-sensitive flow cytometer made possible the analysis of fluorescein biotin lifetimes over a broad range of surface coverage (0.21×10^5 to 9.85×10^5 fluorophores per bead), at a single modulation frequency assuming a single-exponential model. The measured lifetimes were quite insensitive to the extent of surface coverage (as shown by the spectrofluorimetry) until the surface approached saturation. In fact the aggregate lifetimes ($\tau_{av} = \sum_i \alpha_i \tau_i$) as determined via spectrofluorimetry, are in agreement with those determined here. At high surface coverages, most of the fluorescein biotin seem to exhibit nearest-neighbor quenching interactions and shortened lifetimes are resolved.

The general trend which emerges from these measurements is that though ϕ_b varies with coverage, the quenched species are invariably so dim that they make negligible contribution to the intensity detected in the lifetime determination.

C. Binding Kinetics. The kinetic analysis of the binding of fluorescein biotin to beads is complicated by the dependence of ϕ_b on surface density as well as the apparent dependence on time, of the dissociation dynamics. In Figure 7A, curves a, b, and c depict the dissociation kinetics of fluorescein biotin (1.5 nM) initiated 1, 10, and 20 min after mixing of fluorescein biotin with the beads. The curves were fit as double-exponential decays. For the data shown in Figure 7A, the kinetics appear to be increasingly dominated by the slow component (k_{-2}) amplitude, *viz*, 58, 71, and 80% of the a, b, and c, curves, respectively. In addition, dissociative data collected after 1 h of binding (Figure 7B) indicated further gain in stability with $k_{-1} \approx 2.0 \times 10^{-3}$ s^{-1}, $k_{-2} \approx 8.0 \times 10^{-5}$ s^{-1}. For the data shown, we have estimated the half-life for converting to order-of-magnitude slower dissociation kinetics to be less than 3 min.

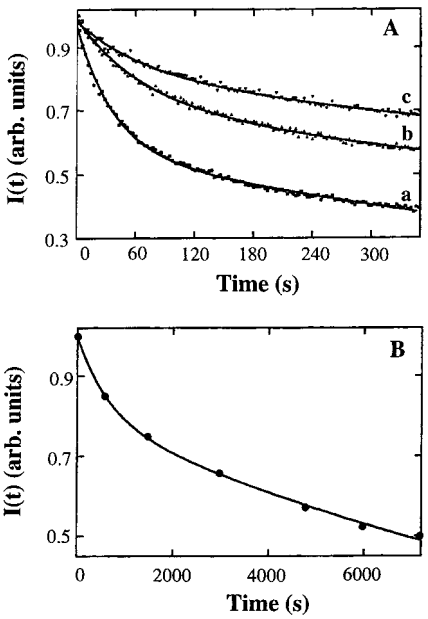

Figure 7. Time-dependent dissociative kinetics on 8×10^6 beads/mL incubated in 1.5 nM fluorescein biotin. (A) Curves a, b, and c represent 1, 10, and 20 min fluorescein biotin incubation times before excess native biotin was added to the beads. The fits to the data produced the following rate constants: (a) $k_{-1} \approx 3.0 \times 10^{-2}$ s^{-1}, $k_{-2} \approx 1.0 \times 10^{-3}$ s^{-1} (b) $k_{-1} \approx 1.0 \times 10^{-2}$ s^{-1}, $k_{-2} \approx 6.0 \times 10^{-4}$ s^{-1} (c) $k_{-1} \approx 1.1 \times 10^{-2}$ s^{-1}, $k_{-2} \approx 5.0 \times 10^{-4}$ s^{-1}. The slow component (k_{-2}) amplitude is dominant, being 58, 71, and 80% of the a, b, and c curves respectively. (B) Dissociation kinetics after 1 h of incubation: $k_{-1} \approx 2.0 \times 10^{-3}$ s^{-1} and $k_{-2} \approx 8.0 \times 10^{-5}$ s^{-1}. The relative amplitudes of k_{-1} and k_{-2} are 20% and 80%, respectively.

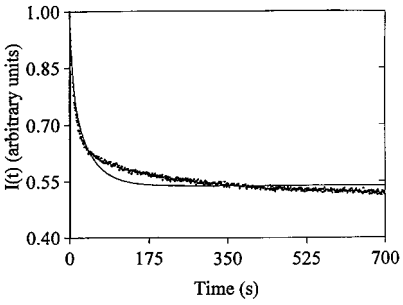

Figure 8. Time-dependent model of spectrofluorimetric binding kinetics. The calculations show a poor theoretical fit to binding data for $[L]_0 = 1.75$ nM and $[S]_0 = 13$ nM using the model:

$$L + S \underset{k_{-1}}{\overset{k_1}{\rightleftharpoons}} LS_1 \underset{k_{-2}}{\overset{k_2}{\rightleftharpoons}} LS_2$$

This model assumes a single binding site and that once bound the system undergoes conformational change to a more stable form. The fit yields rates of $k_1 \sim 5.1 \times 10^6$ M^{-1} s^{-1}, $k_{-1} \sim 0.02$, $k_2 \sim 0.001$ s^{-1}, and $k_{-2} \sim 0.0008$ s^{-1}.

The apparent time dependence of the dissociation rate constants thus leads to a limiting model based on the association of the ligand (L) and binding site (S) to form a complex with an initially labile conformation (LS_1) followed by increasingly stable conformations (LS_n). Our attempts to evaluate a two-state model (Figure 8) resulted in a systematic error in the fit. The failure of this model may be due to the heterogeneous nature of the receptor sites as well as the capacity of fluorescein biotin to bind both its biotin and fluorescein groups (see Figure 11 and Discussion below).

A model which appears to give a reasonable account of the binding and dissociation kinetics is one described in eq 4. The model depends on ϕ_b as an indicator of bound ligand *(vide*

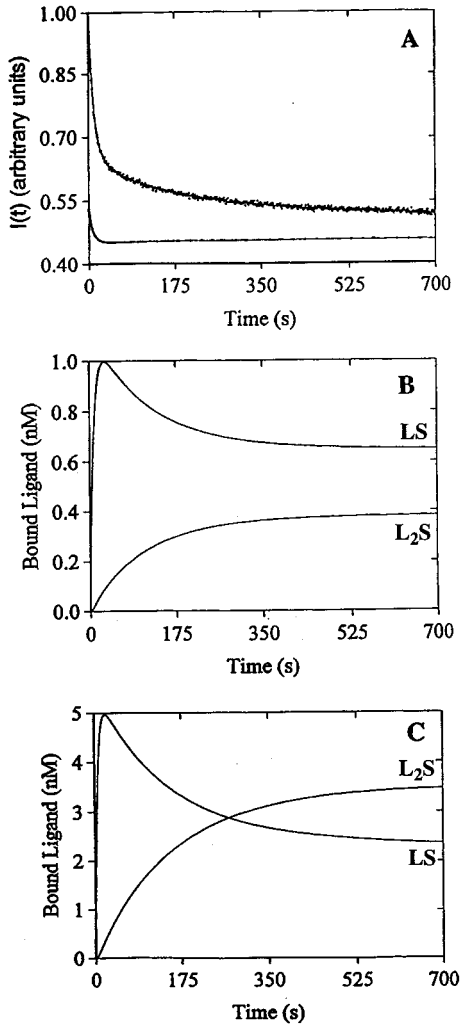

Figure 9. Occupancy-dependent model of spectrofluorimetric binding kinetics. (A) The calculation shows a representative theoretical fit to binding data for $[L]_0 = 1.75$ nM and $[S]_0 = 6.5$ nM; ($k_1 = (1.3 \pm 0.3) \times 10^7$ M^{-1} s^{-1}, $k_2 = (4.0 \pm 1.0) \times 10^6$ M^{-1} s^{-1}, and $k_{-1} = 0.04 \pm 0.01$ s^{-1}, $k_{-2} = 0.003 \pm 0.001$ s^{-1}). Lower curve represents the evolution of ϕ_b with binding. (B) Representative partitioning of bound ligand (LS, L_2S) implied by the theoretical fit at low ligand concentration $[L]_0 = 1.75$ nM and $[S]_0 = 6.5$ nM; LS dominates. (C) At high ligand concentrations, ($[L]_0 = 17.5$ nM and $[S]_0 = 6.5$ nM) [LS] and [L_2S] are comparable.

supra). The following summary account is concerned with theoretical fits to spectrofluorimetric data (cf. Figure 3) from experiments conducted with fluorescein biotin solutions ($[L]_0 = 1.75$, 3.0, and 17.5 nM). The results are presented here while the rationale of the model is deferred to the Discussion. Thus, Figure 9 shows a kinetic fit according to eq 4. Figure 9A depicts typical changes associated with binding of fluorescein biotin (1.75 nM) to beads, including a theoretical fit (top curve) and the corresponding evolution of ϕ_b (estimated from eq 7) as the ligand binds. Figure 9B,C model, the kinetic progress and the relative concentrations of LS and L_2S as a result of the mixing 8×10^6 beads/mL, $[S]_0 = 6.5$ nM, with $[L]_0 = 1.75$ and 17.5 nM. The rate constants fitting the data depend somewhat on the initial concentration of fluorescein biotin: $k_1 = (1.3 \pm 0.3) \times 10^7$ M^{-1} s^{-1} , $k_2 = (0.4 \pm 0.1)$ to $(4.0 \pm 1.0) \times 10^6$ M^{-1} s^{-1}, $k_{-1} = 0.02 \pm 0.01$ to 0.05 ± 0.02 s^{-1}, $k_{-2} = 0.003 \pm 0.001$ to 0.005 ± 0.002 s^{-1}. The noticeably smaller value of k_2 is associated with 17.5 nM fluorescein biotin. It is, however, gratifying to note that the equilibrium constant constants which arise from the ratios of k_1/k_{-1} and k_2/k_{-2} are not only of very similar magnitude but are also equal to the equilibrium constant (4.3×10^8 M^{-1}) obtained from the centrifugation assay.

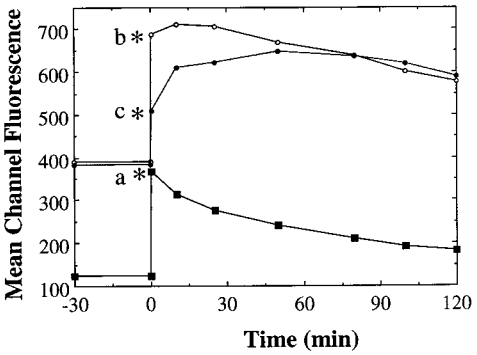

Figure 10. Effect of adding excess native biotin to fluorescent beads with about (a) 1.9×10^5 (b) 5.8×10^5, and (c) 9.9×10^5 fluorophores/bead, respectively, more than 1 h after the initial exposure to fluorescein biotin. The asterisks represent the initial increase in fluorescence intensity a few seconds after addition of native biotin. Subsequently: (a) loses intensity monotonically as fluorescein biotin is replaced with native biotin. (b) and (c) show increasing intensity beyond initial rise as depletion of fluorescein biotin alleviates self-quenching. This is followed by decreasing intensity as more fluorophore is replaced with native biotin.

D. Surface Coverage and Spectroscopic Implications of Ligand Dissociation. After incubation times of fluorescein biotin of more than an hour, exposure to native biotin results in an immediate *increase* (Figure 10) in fluorescence from the beads rather than a loss of intensity as shown in Figure 7. This unquenching process has been reported to occur in less than 25 ms[40] when the probe BODIPY [27] conjugated to avidin is similarly treated with native biotin. This is likely the result of a native biotin molecule replacing the fluorescein moiety of fluorescein biotin in one binding pocket, while the biotin moiety remains firmly attached to another. We note that because the process by which fluorescein unquenches is over in milliseconds, it is essentially complete before appreciable dissociation occurs. The relative initial increases in intensity depend on the extent of surface occupancy at the time of addition of native biotin. The curves (a, b, and c) shown in Figure 10 represent samples incubated in 3, 10, and 100 nM fluorescein biotin solutions. Based on the centrifugation assay, this roughly represents, surface coverages of 1.9×10^5, 5.8×10^5, and 9.9×10^5 fluorophores/bead, respectively. The initial jump in fluorescence at maximum coverage (curve c) is markedly lower, than that observed for the lower coverage samples. Intensity readings taken up to 2 h after the addition of native biotin also displayed an interesting dichotomy at low and high surface coverage. At the lowest surface coverage (curve a), the beads exhibited a monotonic loss in intensity, consistent with the replacement of entire fluorescein biotin molecules with native biotins, whereas with curve b a slight increase in intensity was observed after 20 min before the beads began to slowly lose intensity. The fully covered beads continued to gain intensity after the initial increase for an hour before the onset of decreased intensity.

Discussion

We began this study in order to better define the receptor surfaces of 6.2 μm diameter streptavidin-coated polystyrene beads in anticipation of their use as platforms for biosensors. The characterization requires determination of site number, binding and dissociation rate constants, and spectrofluorometric analysis of binding interactions. We used a combination of flow cytometric and centrifugation/fluorimetric approaches. We

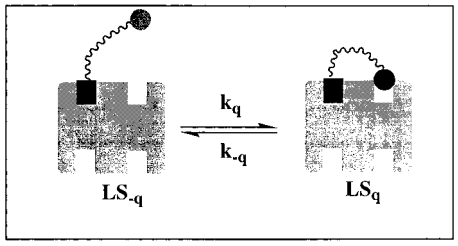

Figure 11. Ostrich[48] quenching model for fluorescein biotin bound to streptavidin in solution, or at low surface density on beads. $k_{-q} \geq 40$ s^{-1}. [40] The relative emission yield of the bound species can be used to determine the magnitude of k_q using the following relationship: $[LS_q]/[LS_{-q}] = k_q/k_{-q} = (1 - \phi_b)/\phi_b$ (8). Equation 8 assumes LS_q to be fully quenched. See text for details.

estimate the site number to be ~1 million per bead from centrifugation measurements (Figure 5). The quenching of the bound fluorescence was strongly dependent on the surface density of the ligand, increasing from about 50% at low density to 80% or more at saturation (Figure 5D). We attribute the quenching at low surface density to a fluorophore/streptavidin interaction[27,41] and the quenching at high surface density to a fluorophore−fluorophore interaction within multivalent streptavidin structures. The quenching was associated with a somewhat reduced fluorescence lifetime measured by time-resolved flow cytometry (Table 3). Kinetic binding analyses are shown in Figures 7−9 and are biphasic in nature. The primary forward rate constant was ~10^7 M^{-1} s^{-1}, a similar order of magnitude as the binding of small ligands to cell surface receptors.[9] A secondary binding rate constant was found to be dependent on the initial ligand concentration, and varied by an order of magnitude range. The dissociation rate constant(s) was strongly time dependent, with rates as large as 0.05 s^{-1} shortly (seconds to minutes) after ligand binding and was determined to decrease with ligand binding time, manifested by the onset of biphasic kinetics. The effects of surface coverage on the emission quantum yield, binding kinetics and stability are explored below.

A. Binding, Quenching, and Surface Coverage. The observations and interpretation presented here are based on the quenching of fluorescence upon binding of fluorescein biotin to streptavidin in solution or on bead surfaces. Therefore, it is convenient to begin the discussion by commenting on the quenching mechanism.

1. Primary Quenching. Elsewhere,[27,37,40,41] it has been reported that fluorescein as well as other fluorescent dyes are significantly quenched when conjugated to streptavidin. The loss in intensity has been attributed to contact between the fluorophore and amino acid residues within the protein's binding pocket.[41] The enhancement of fluorescence in the presence of native biotin is corroborating evidence for such interaction.

In Figure 11, the diffusive encounter between fluorescein biotin and streptavidin (eq 4a) leads to the relatively nonfluorescent species (LS_q). The quasi-unimolecular process of receptor binding, $k_1[S]_0$, is much slower than k_q.[42] Thus, the overall quenching process only depends on the diffusion-limited process. In the simplest limit, the emission quantum yield of LS_q is assumed to be negligible. In order to verify this assumption, we turn to the polarization experiments. When excess streptavidin ($[S]_0 = 272$ nM) is mixed with 1.5 nM fluorescein biotin, only 10% of the original fluorescence remains (Figure 6A). Based on the equilibrium constant for binding in solution, it is likely that the amount of free ligand is negligible. Thus, the bound species exist as a mixture of LS_q and LS_{-q}, dominated by the LS_q (i.e., solution is composed of 90% reletively nonfluorescent LS_q). Luminescence from LS_q, if present, would be expected to polarize the emission more than LS_{-q} because, (a) the bound fluorescein moiety has fewer degrees of rotational freedom than the free and (b) polarization is inversely related to the lifetime[33] ($\tau_{LR_{-q}} > \tau_{LR_q}$). In the presence of native biotin the bound species are permanently converted to 100% LS_{-q} with a polarization value of 0.2, whereas a polarization value of 0.12 is determined for the mixture. We thus conclude that the 10% residual luminescence originates solely from LS_{-q}. This view is also consistent with excited state lifetime measurements, which show the 10% residual fluorescence lifetime as being largely similar to that of the free (see footnote *b* in Table 3). The reduced polarization ($P = 0.12$) was unexpected and is not readily explained. That it is less than that for neat LS_{-q} could conceivably be related to the dynamics associated with the quenching and unquenching processes, which are blocked in the presence of native biotin.

2. Surface Coverage and Quenching. The accumulation of fluorescein biotin on a bead is accompanied by a decline of the emission quantum yield of the bound species (Figure 5D). At low surface coverage, the recovery in fluorescence, caused by the introduction of native biotin, is higher than at high surface density (Figure 10). This behavior offers important clues regarding the topographical makeup of the receptor surface. At low coverage, the receptor to fluorophore ratio is high enough to accommodate random binding of the fluorescein as well as the biotin moiety (LS_q process is favored). However, in contrast to solution binding where 90% of the flourophore's emission yield is quenched, only ≈50% loss in emission intensity is observed upon binding to beads. This could be a result of the random orientation of receptor pockets at the surface (Figure 1) where formation of LS_q is restricted, so that only 50% of the binding sites have adjacent cis sites which enable "ostrich" binding (Figure 11). Alternatively, surface attachment could alter the rates of k_q and k_{-q}. At higher coverages, the mode of quenching gradually incorporates that associated with the formation of nonfluorescent nearest-neighbor aggregates.[43] It is also clear from Figure 1 that some binding sites may not be as readily accessible to incoming ligands as others. This may have consequences which are manifested in the kinetics of binding at low and high ligand concentrations *(vide infra).* From the viewpoint of intensity measurements being dependent on coverage, at low ligand concentrations, nonadjacent and easily accessible sites are randomly occupied first, and quenching is mainly via fluorophore contact with a binding pocket. The onset of surface saturation of multivalent streptavidins is marked with nearest-neighbor quenching.

The conceptual view of self-quenching aggregates at high surface coverage is consistent with the dependence of ϕ_b on surface occupancy (Figure 5D). This is corroborated by data shown in Figure 10. When native biotin is added to the ligand-saturated beads, the beads undergo the least increase in fluorescence since they have the fewest number of sites available for capturing the fluorescein moiety. Minutes to 2 h subsequent to the addition of native biotin, the competitive replacement of the fluorophore by native biotin is marked by a loss in intensity in sample a (1.9×10^5 fluorophores/bead) and an initial gain and then loss in intensity in b and c (5.8×10^5, and 9.9×10^5 fluorophores/bead, respectively). For sample a, with little to no nearest-neighbor interactions, the loss in intensity is as expected. However, at high surface density, where ϕ_b is also a result of nearest-neighbor interactions, each fluorophore competed off by native biotin results in a brighter remnant fluorophore. Thus, the dissociation of fluorescein biotin at high surface coverage

must result in increased intensity until all interacting neighbors are depleted.

B. Binding and Dissociation Kinetics. From a mechanistic viewpoint, the complexity of the binding of fluorescein biotin to receptor sites on beads is characterized by values of ϕ_b which depend on occupancy. Once bound, the biotin/streptavidin linkage is easily labile in the first few seconds (Figure 7) and appears to gain stability in the ensuing minutes. In previous studies, multiphasic dissociation kinetics have been observed for biotin[14,44] and its conjugates.[28,37,45,46] This phenomenon has been previously attributed to streptavidin existing in forms of varying affinity as initially reported by Green[14] and could result from progressive ligand association with the highest affinity molecules. Alternatively, and in contrast to solution behavior, there could be a stabilization of binding through a slow ligand-induced conformational change similar to that recently reported for the insulin receptor.[47]

We attempted to fit the association kinetics with a simple time-dependent model (Figure 8). Because the model appeared to yield systematic error in the fit, we thus turned to an alternate model (eq 4) which relies on the dependence of ϕ_b on surface coverage. The dependence of ϕ_b on occupancy (Figure 5D) is empirically represented by eq 7. In the simplest limit, the evolution of ϕ_b with time (and thus occupancy) represents quenching which is initially dominated by that of ostrich quenching (Figure 11) which is gradually supplanted by near-neighbor interactions (generalized as L_2R in eq 4). Because the contributions to ϕ_b of ostrich and near-neighbor interations are not resolved, ϕ_b is suited for the phenomenological binding model. The evolution of intensity requires an expanded form of eq 3 which delineates LS and L_2S as shown in eq 9.

$$\frac{I_t}{I_0} = \frac{[L]_t}{[L]_0} + \phi_b \frac{[LS]_t}{[L]_0} + 2\phi_b \frac{[L_2S]_t}{[L]_0} \qquad (9)$$

The binding kinetics for any given $[L]_0$ are interpreted in terms of the velocity equations which arise from eq 4 with typical results shown in Figure 9. As the kinetic data thus analyzed shares almost similar incubation times as the dissociation kinetics shown in curve a in Figure 7; the agreement between dissociation rate constants of Figure 7a and those derived from this model are notable.

The apparent dependence of the secondary rate constant (k_2) on concentration could result from two factors. First, there is competition for binding sites between incoming ligands and the fluorescein moiety of ostrich bound ligands. k_2 is thus likely to be reduced by a factor of 9 based on estimates using eq 8 (Figure 11) and solution quenching data.[42] Second, because of the random nature in which the streptavidins are oriented on the surface, some sites may be less accessible than others and are thus only occupied at high $[L]_0$ and thus the lower values of k_2 with increasing $[L]_0$. such factors would explain the failure of the time-dependent model (Figure 8). We have not attempted to build the time dependence into this model.

C. Stability. Most literature discussions on the interactions of biotin/streptavidin systems emphasize the extremely large binding constant $\approx 10^{13}$ M^{-1} of native biotin and streptavidin which is controlled by an exceptionally slow dissociation rate in solution.[12,14,17,19,20,29] However, as was first reported by Chignell *et al.*,[29] bulky spin-labeled biotin derivatives had binding affinities much less than 10^{13} M^{-1}. The strength of the biotin−streptavidin bond has been attributed to extensive hydrogen bonding between the ureidic ring and the carboxyl oxygens of biotin and protein groups.[13,15−18] The virtually irreversible binding process is facilitated by the combined rearrangements of particular amino acid residues within the binding pocket and ligand motions outside of the binding pocket.[12] Functionalization of biotin leads to the loss of one of the carboxylic oxygens, thus losing some hydrogen-bonding potential. However, the major loss in affinity is likely to arise from the steric bulk[15] which inhibits the ability of biotin to settle in the most stable position inside the binding pocket. Furthermore, bulky substituents are likely to inhibit paired binding at cis sites on streptavidin. The streptavidin tetramer has D_2 symmetry, where adjacent binding sites are separated by ≈20 Å.[16,18] Steric constraints on biotin conjugates are thus defined by this separation distance of binding pockets, where bivalent binding potential may be tenuous for bulky biotinyl ligands.[19] Fluorescein biotin, used in this work, extends >25 Å long. One may envision interligand steric bulk to be an obstacle to paired binding, a factor which may contribute to the high dissociative rates at early times. However, as our data (Figures 7 and 9) shows, the stability of the fluorescein biotin/streptavidin complex appears to evolve with time; thus the dissociation dynamics span 3 orders of magnitude as the rate constants decrease with incubation time.

D. Summary and Conclusions. In this study we have demonstrated that the beads used here are a viable platform for the study of streptavidin−biotin for use in biosensing or bioanalytical applications. The bead-bound receptors bind to fluorescein biotin with high affinity and long-term stability. However, at least two caveats have emerged from this study. First, the high stability associated with the streptavidin/biotin interaction is not instantaneous, but gains stability over some time. Second, conjugation of biotin to bulky groups invariably leads to loss of affinity, and thus the expectation of stability equaling that of native biotin is not tenable. High surface coverages have the undesirable property that the fluorophores exhibit self-quenching. Thus, the coverage is best kept small. For practical applications, the fluorescence of bound ligand may be optimized by the addition of native biotin after equilibrium incubation of the biotinylated fluorophore.

Acknowledgment. This work was supported by the Department of Defense through the Multidisciplinary Research Program of the University Research Initiative (Office of Naval Research) grant N00014-95-1-1315), through NIH RR-01315 to the National Flow Cytometry Resource, and the UNM Cancer Center by the NM State Cigarette Tax. We acknowledge useful discussions with Drs. Ralph Young (Rochester, NY), David Dunlap (Physics Dept. UNM), and Pete Simons (UNM HSC).

References and Notes

(1) Paddle, B. M. *Biosens. Bioelectron.* **1996**, *11*, 1079−1113.
(2) Nolan, J. P.; Shen, B. H.; Park, M. S.; Sklar, L. S. *Biochemistry* **1996**, *35*, 11668−11676.
(3) Chen, C.; Wagner, H.; Still, W. C. *Science* **1998**, *279*, 851−853.
(4) Lam, K. S.; Lebl, M.; Krchnak, V. *Chem. Rev.* **1997**, *97*, 411−448.
(5) Ohlmeyer, M. H. J.; Swanson, R. N.; Dillard, L. W.; Reader, J. C.; Asouline, G.; Kobayashi, R.; Wigler, M.; Still, W. C. *Proc. Natl. Acad. Sci. U.S.A.* **1993**, *90*, 10922−10926.
(6) Still, W. C. *Acc. Chem. Res.* **1996**, *29*, 153−163.
(7) Sklar, L. A.; Finney, D. A.; Oades, Z. G.; Jesaitis, A. J.; Painter, R. G.; Cochrane, C. G. *J. Biol. Chem.* **1984**, *259*, 5661−5669.
(8) Sklar, L. A.; Oades, Z. G.; Jesaitis, J.; Painter, R. G.; Cochrane, C. G. *Proc. Natl. Acad. Sci. U.S.A.* **1981**, *78*, 7540−7544.
(9) Fay, S. P.; Posner, R. G.; Swann, W. N.; Sklar, L. A. *Biochemistry* **1991**, *30*, 5066−5075.
(10) Huang, S.; Stump, M. D.; Weiss; Caldwell, K. D. *Anal. Biochem.* **1996**, *237*, 115−122.
(11) Sicchierolli, S. M.; Carmona-Ribeiro, A. M. *J. Phys. Chem.* **1996**, *100*, 16771−16775.

(12) Chilkoti, A.; Stayton, P. S. *J. Am. Chem. Soc.* **1995**, *117*, 10622−10628.

(13) Gonzalez, M.; Bagatolli, L. A.; Echabe, I.; Arrondo, J. L. R.; Argarana, C. E.; Cantor, C. R.; Fidelio, G. D. *J. Biol. Chem.* **1997**, *272*, 11288−11294.

(14) Green, N. M. *Biochem. J.* **1963**, *89*, 585−591.

(15) Hendrickson, W. A.; Pahler, A.; Smith, J. L.; Satow, Y.; Merritt, E. A.; Phizackerley, R. P. *Proc. Natl. Acad. Sci. U.S.A.* **1989**, *86*, 2190−2194.

(16) Pugliese, L.; Coda, A.; Malcovati, M.; Bolognesi, M. *J. Mol. Biol.* **1993**, *231*, 698−710.

(17) Weber, P. C.; Ohlendorf, D. H.; Wendoloski, J. J.; Salemme, F. R. *Science* **1989**, *243*, 85−88.

(18) Weber, P. C.; Wendoloski, J. J.; Pantoliano, M. W.; Salemme, F. R. *J. Am. Chem. Soc.* **1992**, *114*, 3197−3200.

(19) *Methods in Enzymology*; Wilchek, M., Bayer, E. A., Eds.; Academic Press: London, 1990; Vol. 184, pp 51−67.

(20) *Methods in Enzymology*; Wilchek, M., Bayer, A. B., Eds.; Academic Press: London, 1990; Vol. 184, pp 123−138.

(21) Wilchek, M.; Bayer, E. A. *Anal. Biochem.* **1988**, *171*, 1−32.

(22) Siegmund, H.; Becker, A. *Sensors Actuators B* **1993**, *11*, 103−108.

(23) Shinohara, Y.; Sota, H.; Kim, F.; M., S.; Gotoh, M.; Tosu, M.; Hasegawa, Y. *J. Biochem.* **1995**, *117*, 1076−1082.

(24) Nilsson, P.; Persson, B.; Uhlen, M.; Nygren, P. *Anal. Biochem.* **1995**, *224*, 400−408.

(25) Komives, C.; Schultz, J. S. *Talanta* **1992**, *39*, 429−441.

(26) Spherotech "SpherotechTECHNICAL Notes-1 (STN1)," Spherotech Inc, Libertyville, IL, 1998.

(27) Haugland, R. P. *Handbook of Fluorescent Probes and Research Chemicals*, 6th ed.; Molecular Probes: Eugene, OR, 1996.

(28) Zhao, S.; Reichert, W. M. *Langmuir* **1992**, *8*, 2785−2791.

(29) Chignell, C. K.; Starkweather, D. K.; Sinha, B. K. *J. Biol. Chem.* **1975**, *250*, 5622−5630.

(30) Buranda, T.; Lopez, G. P.; Keij, J.; Harris, R.; Sklar, L. A. *Cytometry*, in press.

(31) Murphy, R. F. In *Flow Cytometry and Sorting*; Lindmo, T., Mendelsohn, M., Eds.; Wiley-Liss, Inc.: New York, 1988; pp 355−366.

(32) Roitt *Essential Immunology*, 8th ed.; Blackwell Scientific Publications: Oxford, UK, 1994.

(33) Lakowicz, J. R. *Principles of Fluorescence Spectroscopy*; Plenum Press: New York, 1983.

(34) Steinkamp, J. A.; Yoshida, T. M.; Martin, J. C. *Rev. Sci. Instrum.* **1993**, *64*, 3440−3450.

(35) Deka, C.; Sklar, L. A.; Steinkamp, J. A. *Cytometry* **1994**, *17*, 94−101.

(36) Deka, C.; Lehnert, B. E.; Lehnert, N. M.; Jones, G. M.; Sklar, L. A.; Steinkamp, J. A. *Cytometry* **1996**, *25*, 271−279.

(37) Gruber, H. J.; Marek, M.; Schindler, H.; Kaiser, K. *Bioconjug. Chem.* **1997**, *8*, 552−559.

(38) Schray, K. J.; Artz, P. G.; Hevey, C. R. *Anal. Chem.* **1988**, *60*, 853−855.

(39) Szmacinski, H.; Lakowicz, J. R. *Sensors Actuators B* **1996**, *30*, 207−215.

(40) Emans, N.; Biwersi, J.; Verkman, A. S. *Biophys. J.* **1995**, *195*, 716−728.

(41) Barbarakis, M. S.; Smith-Palmer, T.; Bachas, L. G. *Talanta* **1993**, *40*, 1139−1145.

(42) For $k_1 = 1.3 \times 10^7\ M^{-1}\ s^{-1}$ and $[S]_0 = 6.5$ nM; $k_1[S]_0 = 0.08\ s^{-1}$. k_q is determined from eq 8 and Figure 11, to be 360 s^{-1}. This value is rationalized as follows: When streptavidin is added to fluorescein biotin, 90% of the fluorophore is quenched, thus generating a 9:1 ratio of $[LS]_q$ versus $[LS_{-q}]$. k_{-q} is estimated to be at least 40 s^{-1}.

(43) Turro, N. J. *Modern Molecular Photochemistry*; Benjamin/Cummings: Menlo Park, CA, 1978; pp 296−321.

(44) Piran, U.; Riordan, W. J. *J. Immunol. Methods* **1990**, *133*, 141−143.

(45) Finn, F. M.; Hofmann, K. H. *Methods Enzymol.* **1985**, *109*, 418−419.

(46) Lavielle, S.; Chassaing, G.; Marquet, A. *Biochim. Biophys. Acta* **1983**, *759*, 270−277.

(47) Lee, J.; Pilch, P. F.; Shoelson, S. E.; Scarlata, S. F. *Biochemistry* **1997**, *36*, 2701−2708.

(48) The ostrich metaphor is from the popular belief that the ostrich, when pursued, hides its head in the sand and believes itself to be unseen. In the context used here it only refers to the fluorescein moiety's foray into the receptor pocket.